

Supplemental Data Part 2

Backscattered SEM Assessment of *Fam83h^{Tr/Tr}*, *Fam83h^{Tr/+}*, & *Fam83h^{+/+}* Mouse Mandibular Incisor Incremental Cross-Sections.

Part 2a: Comparison of Incisor Cross-Sections from the 3 genotypes.

- Fig. S8.** Backscattered SEM images of mandibular incisor cross-sections taken at ~1 mm increments (WT-953; Het-986; Null-X) starting at the apical end of the incisor (low magnification).
- Fig. S9.** Backscattered SEM images of mandibular incisor cross-sections taken at ~1 mm increments (WT-953; Het-986; Null-X) starting at the apical end of the incisor (middle magnification).
- Fig. S10.** Histology of *Fam83h^{+/+}* Maxillary Incisor at 7-weeks (WT17).

Part 2b: *Fam83h^{Tr/+}* Individual Incisor Cross-Sections

- Fig. S11.** Backscattered SEM images of mandibular incisor cross-sections of Het-950 taken at ~1 mm increments starting at the apical end of the incisor.
- Fig. S12.** Backscattered SEM images of mandibular incisor cross-sections of Het-951 taken at ~1 mm increments starting at the apical end of the incisor.
- Fig. S13.** Backscattered SEM images of mandibular incisor cross-sections of Het-952 taken at ~1 mm increments starting at the apical end of the incisor.
- Fig. S14.** Backscattered SEM images of mandibular incisor cross-sections of Het-976 taken at ~1 mm increments starting at the apical end of the incisor.
- Fig. S15.** Backscattered SEM images of mandibular incisor cross-sections of Het-982 taken at ~1 mm increments starting at the apical end of the incisor.
- Fig. S16.** Backscattered SEM images of mandibular incisor cross-sections of Het-986 taken at ~1 mm increments starting at the apical end of the incisor.

Part 2c: *Fam83h^{Tr/Tr}* Individual Incisor Cross-Sections

- Fig. S17.** Backscattered SEM images of mandibular incisor cross-sections of Null-932 taken at ~1 mm increments starting at the apical end of the incisor.
- Fig. S18.** Backscattered SEM images of mandibular incisor cross-sections of Null-956 taken at ~1 mm increments starting at the apical end of the incisor.
- Fig. S19.** Backscattered SEM images of mandibular incisor cross-sections of Null-957 taken at ~1 mm increments starting at the apical end of the incisor.
- Fig. S20.** Backscattered SEM images of mandibular incisor cross-sections of Null-974 taken at ~1 mm increments starting at the apical end of the incisor.
- Fig. S21.** Backscattered SEM images of mandibular incisor cross-sections of Null-995 taken at ~1 mm increments starting at the apical end of the incisor.
- Fig. S22.** Backscattered SEM images of mandibular incisor cross-sections of Null-X taken at ~1 mm increments starting at the apical end of the incisor.

Part 2d: *Fam83h^{+/+}* Individual Incisor Cross-Section

- Fig. S23.** Backscattered SEM images of mandibular incisor cross-sections of Wild-Type-953 taken at ~1 mm increments starting at the apical end of the incisor.

Part 2e: Hardness Testing

- Fig. S24.** Enamel area on 7-week mandibular incisor level 8 (alveolar crest) cross sections.
- Fig. S25.** Microhardness Testing. bSEM images of surfaces tested & Microhardness Table.
- Fig. S26.** Nanohardness Test Table
- Fig. S27.** Nanohardness Testing. SEM images of level 8 cross-sections of 7-week mandibular incisors in *Fam83h^{+/+}* (n=6), *Fam83h^{+/Tr}* (n=6) and *Fam83h^{Tr/Tr}* (n=5) for nanohardness testing.

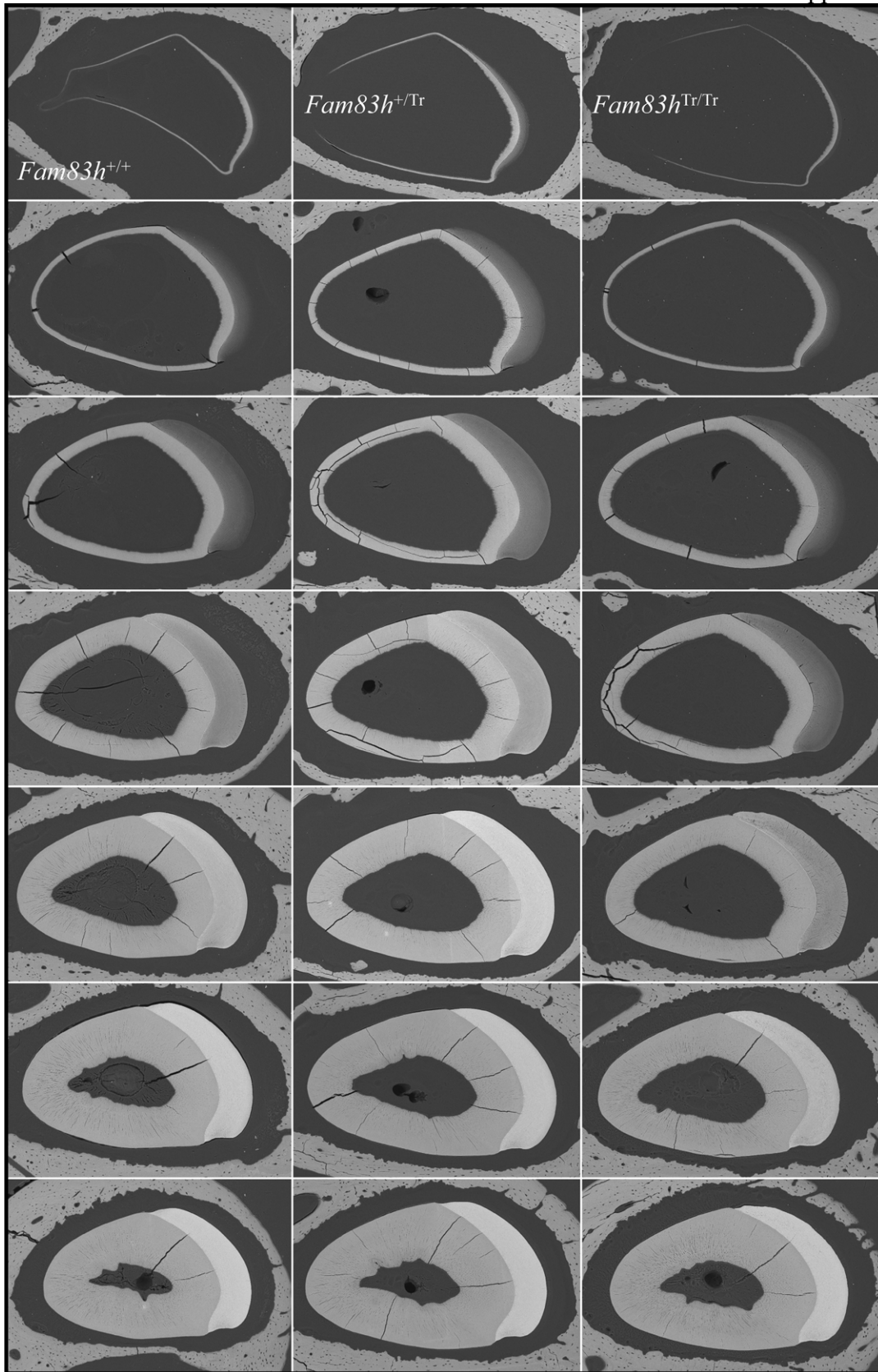


Fig. S8. Backscattered SEM images of mandibular incisor cross-sections taken at ~ 1 mm increments (WT-953; Het-986; Null-X) starting at the apical end of the incisor (low magnification). The top row around the mid-secretory stage. The second row approximates the end of the secretory stage when the enamel layer reaches its final dimensions. Subsequent images show progressive mineralization of the enamel layer during the maturation stage.

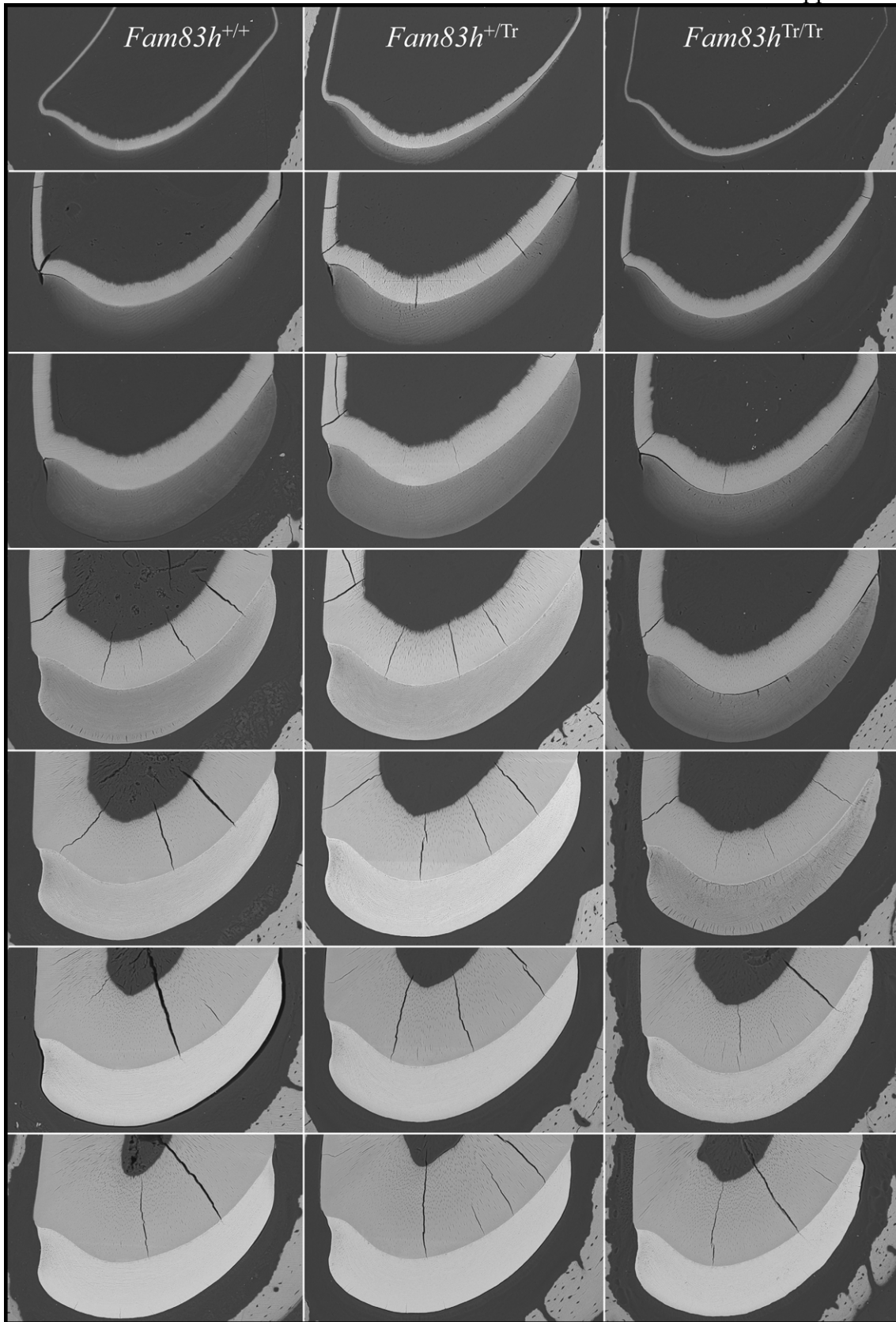


Fig. S9. Backscattered SEM images of mandibular incisor cross-sections taken at ~1 mm increments (WT-953; Het-986; Null-X) starting at the apical end of the incisor (middle magnification). The top row around the mid-secretory stage. The second row approximates the end of the secretory stage when the enamel layer reaches its final dimensions. Subsequent images show progressive mineralization of the enamel layer during the maturation stage.

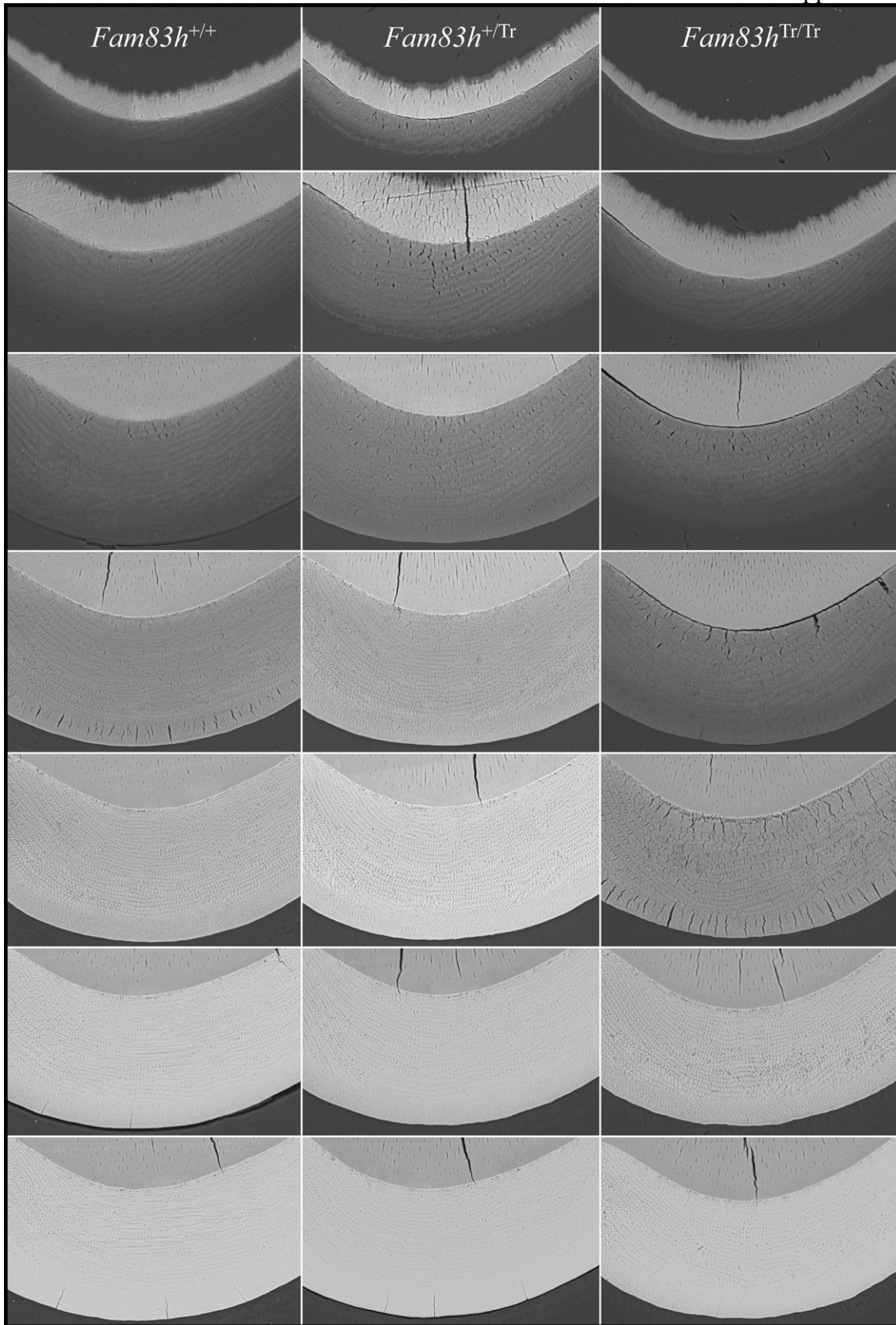


Fig. S10. Backscattered SEM images of mandibular incisor cross-sections taken at ~ 1 mm increments (WT-953; Het-986; Null-X) starting at the apical end of the incisor (high magnification). The top row around the mid-secretory stage. The second row approximates the end of the secretory stage when the enamel layer reaches its final dimensions. Subsequent images show progressive mineralization of the enamel layer during the maturation stage.

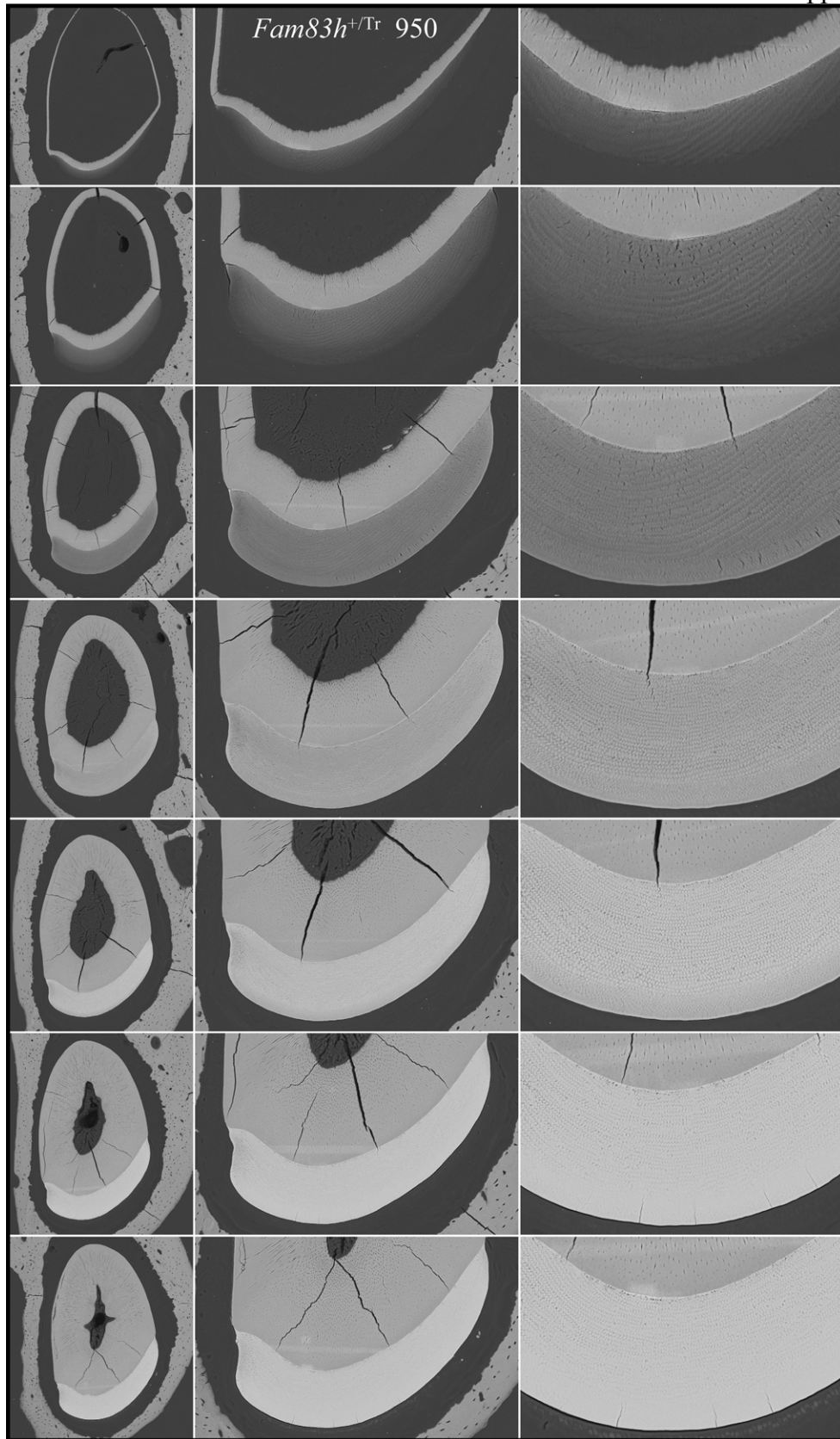


Fig. S11. Backscattered SEM images of mandibular incisor cross-sections of Het-950 taken at ~1 mm increments starting at the apical end of the incisor. The top row around the mid-secretory stage. The second row approximates the end of the secretory stage when the enamel layer reaches its final dimensions. Subsequent images show progressive mineralization of the enamel layer during the maturation stage.

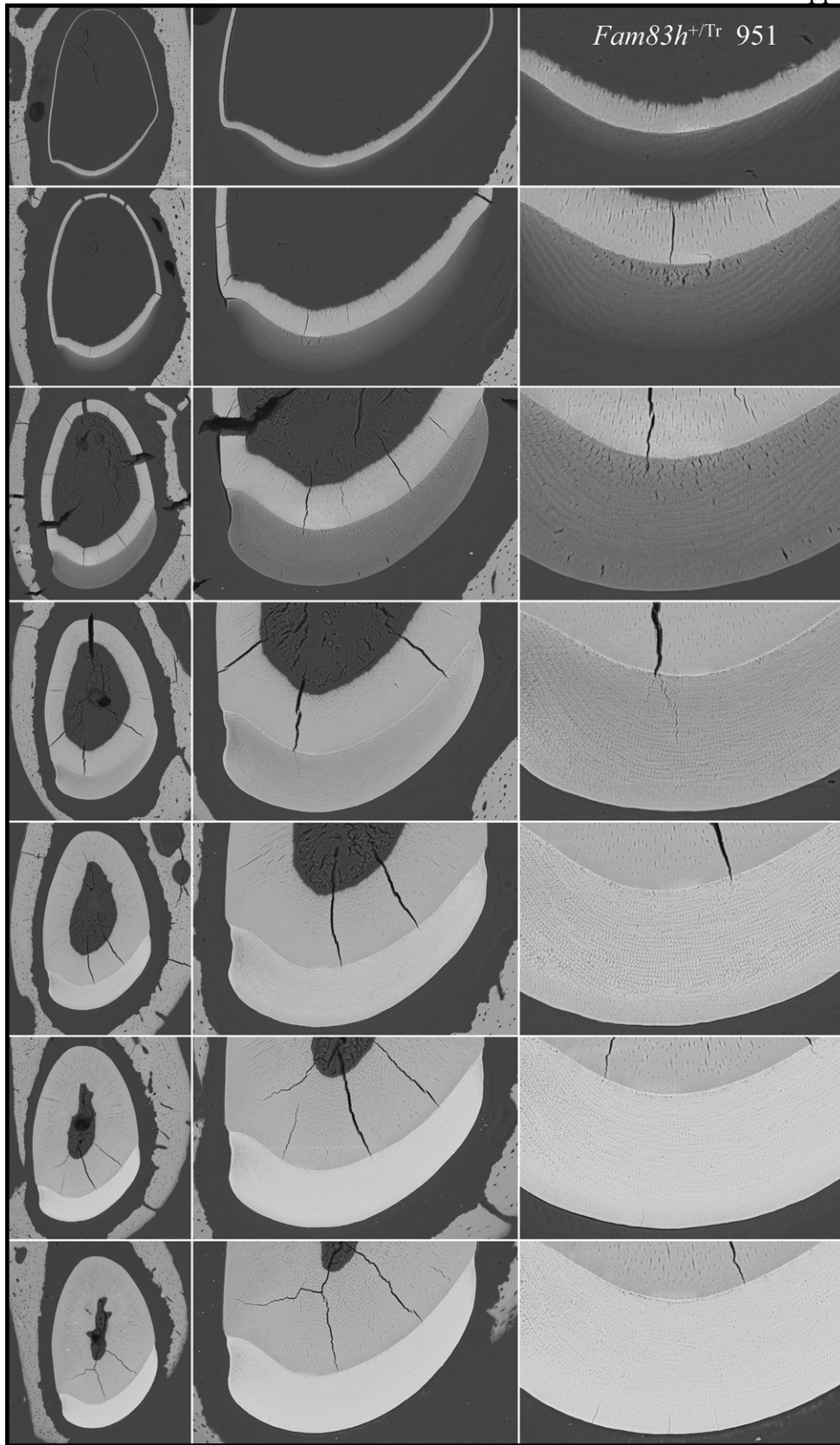


Fig. S12. Backscattered SEM images of mandibular incisor cross-sections of Het-951 taken at ~1 mm increments starting at the apical end of the incisor. The top row around the mid-secretory stage. The second row approximates the end of the secretory stage when the enamel layer reaches its final dimensions. Subsequent images show progressive mineralization of the enamel layer during the maturation stage.

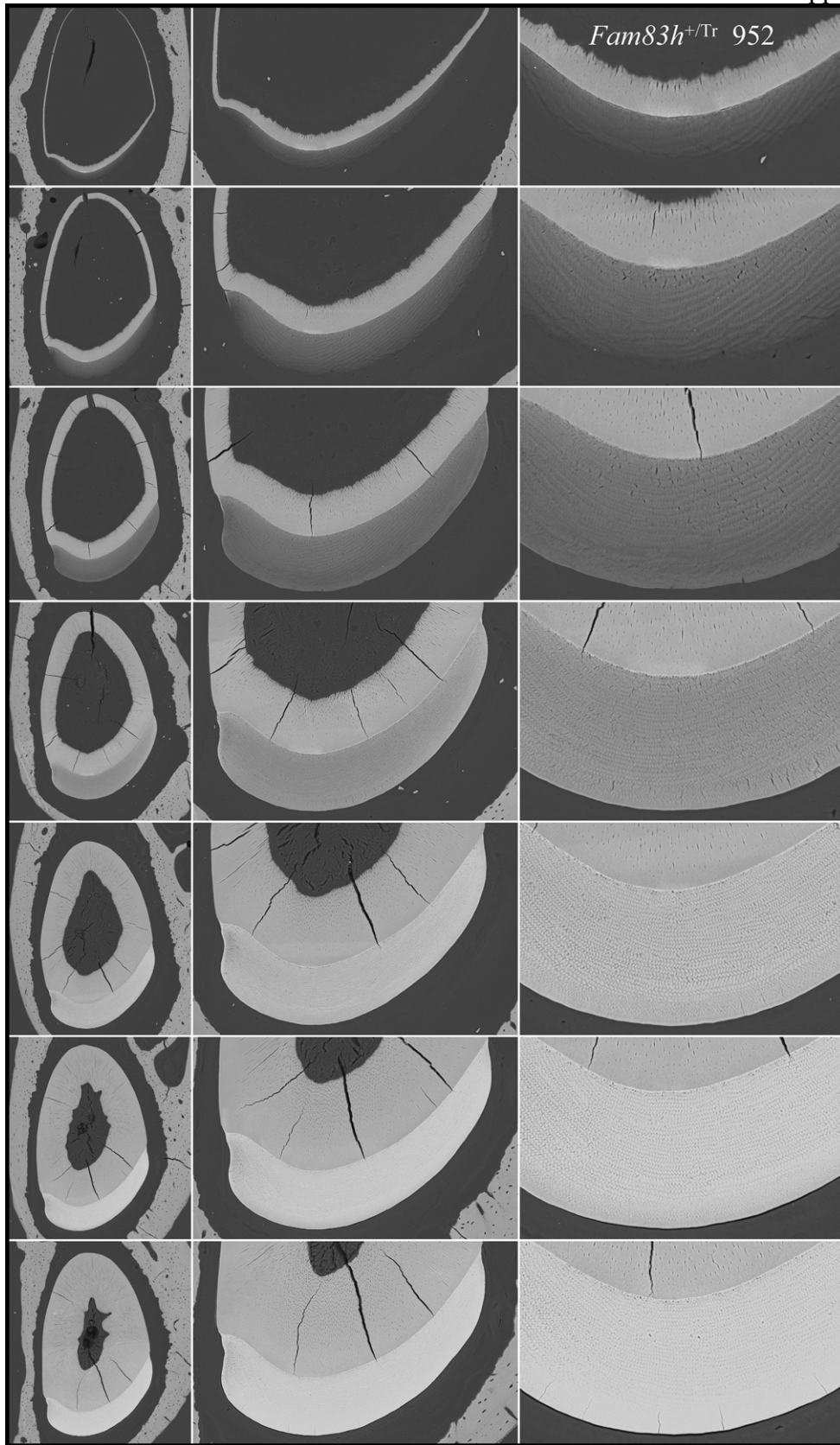


Fig. S13. Backscattered SEM images of mandibular incisor cross-sections of Het-952 taken at ~1 mm increments starting at the apical end of the incisor. The top row around the mid-secretory stage. The second row approximates the end of the secretory stage when the enamel layer reaches its final dimensions. Subsequent images show progressive mineralization of the enamel layer during the maturation stage.

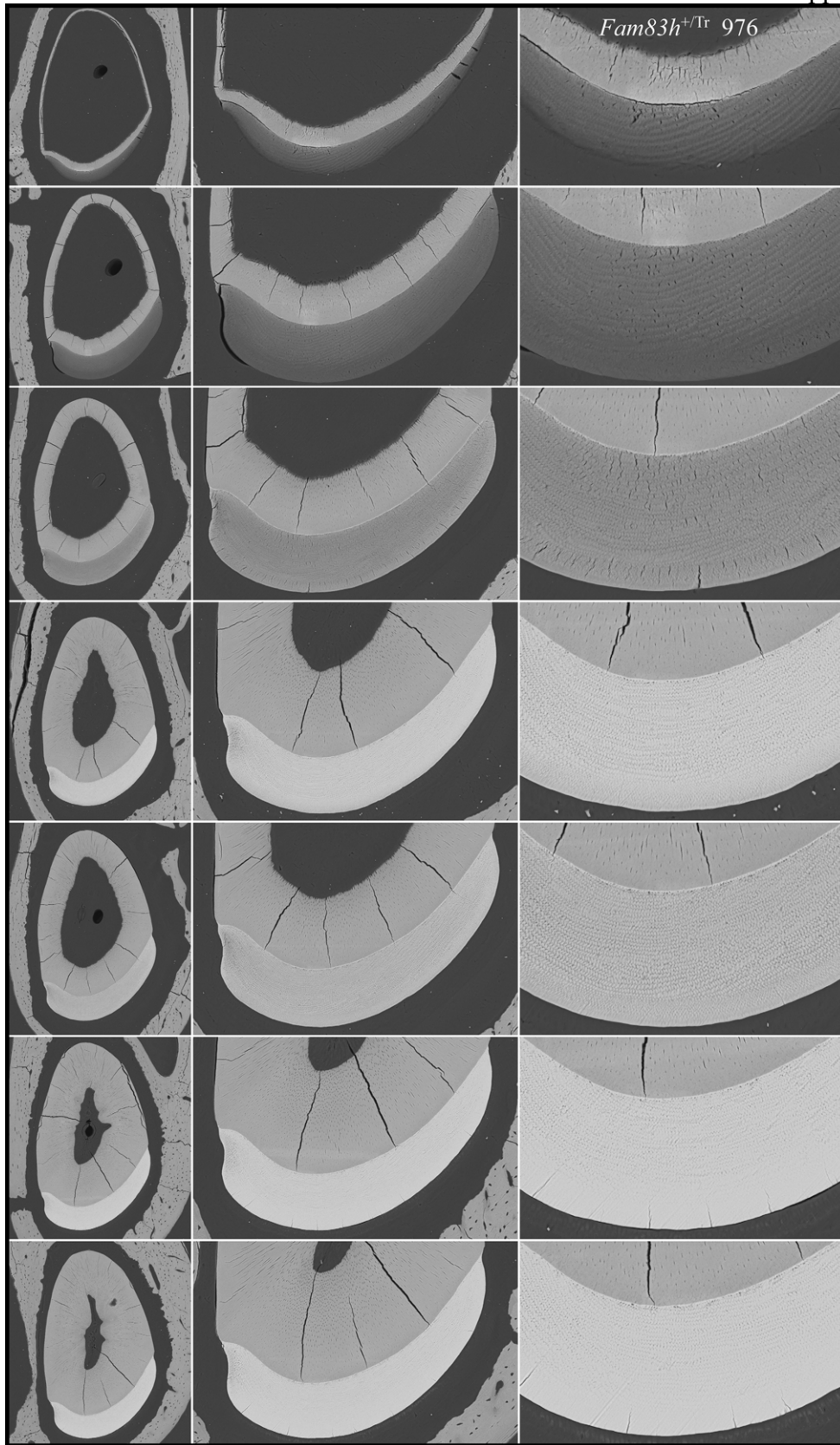


Fig. S14. Backscattered SEM images of mandibular incisor cross-sections of Het-976 taken at ~1 mm increments starting at the apical end of the incisor. The top row around the mid-secretory stage. The second row approximates the end of the secretory stage when the enamel layer reaches its final dimensions. Subsequent images show progressive mineralization of the enamel layer during the maturation stage.

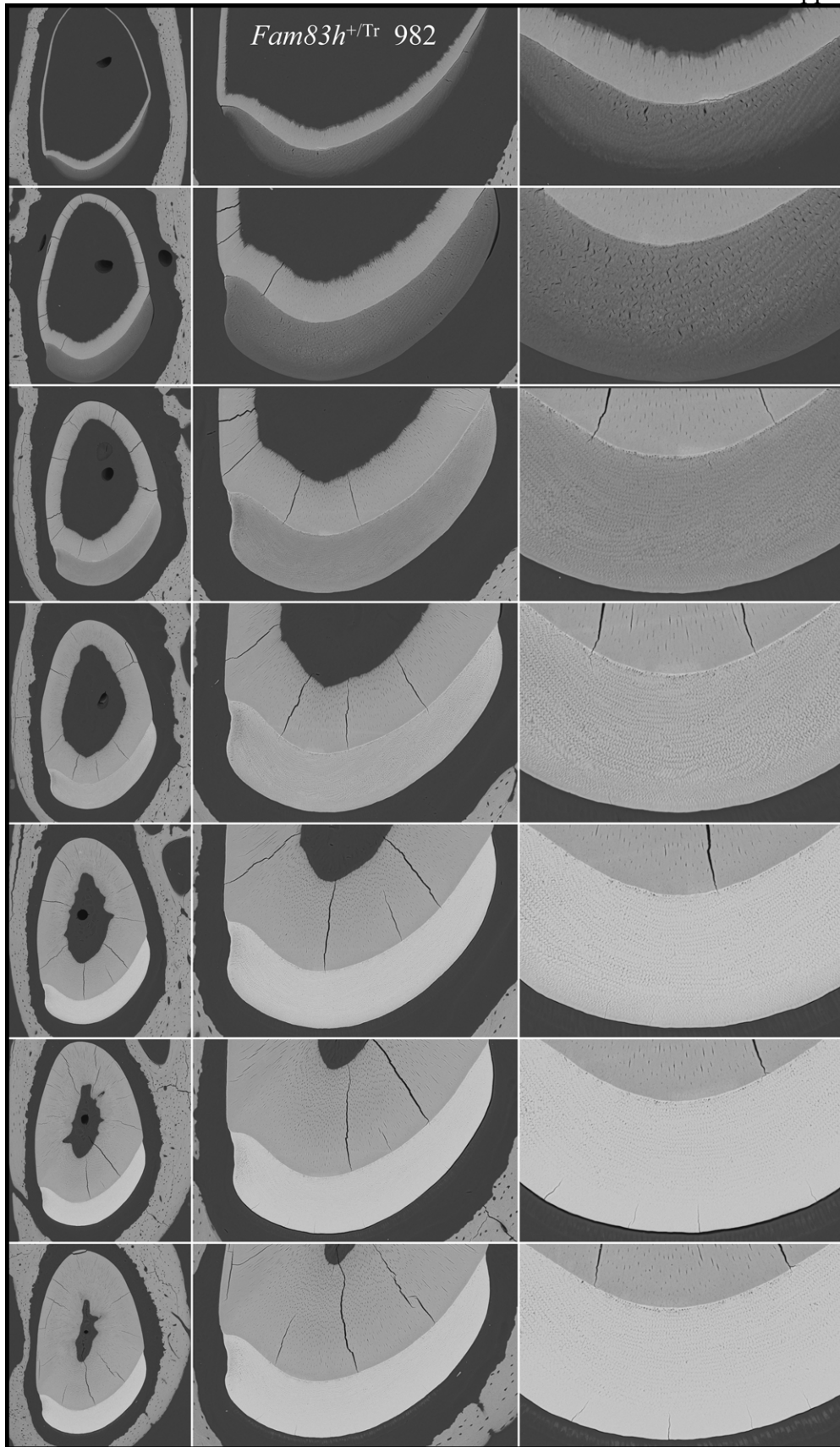


Fig. S15. Backscattered SEM images of mandibular incisor cross-sections of Het-982 taken at ~ 1 mm increments starting at the apical end of the incisor. The top row around the mid-secretory stage. The second row approximates the end of the secretory stage when the enamel layer reaches its final dimensions. Subsequent images show progressive mineralization of the enamel layer during the maturation stage.

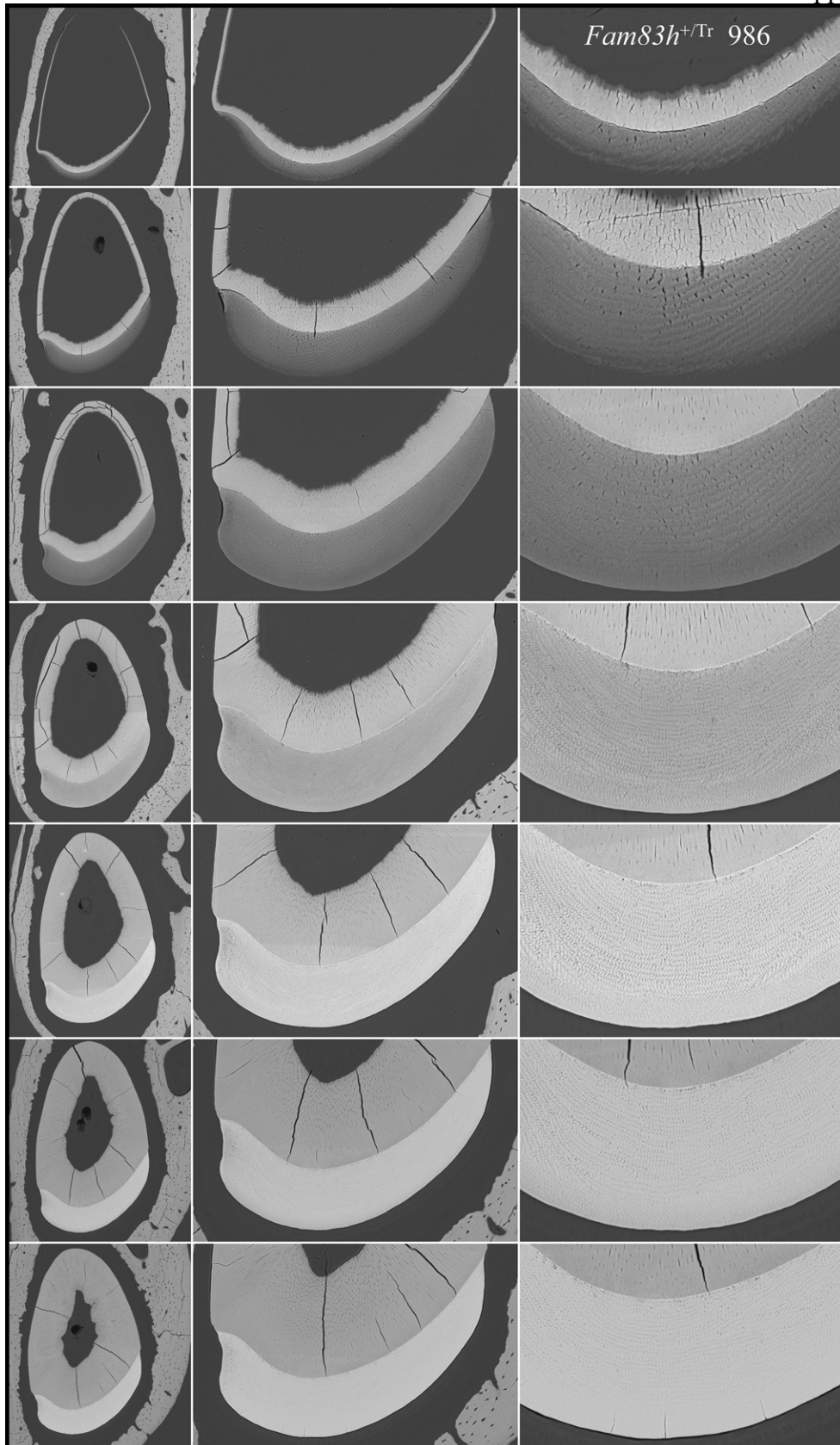


Fig. S16. Backscattered SEM images of mandibular incisor cross-sections of Het-986 taken at ~1 mm increments starting at the apical end of the incisor. The top row around the mid-secretory stage. The second row approximates the end of the secretory stage when the enamel layer reaches its final dimensions. Subsequent images show progressive mineralization of the enamel layer during the maturation stage.

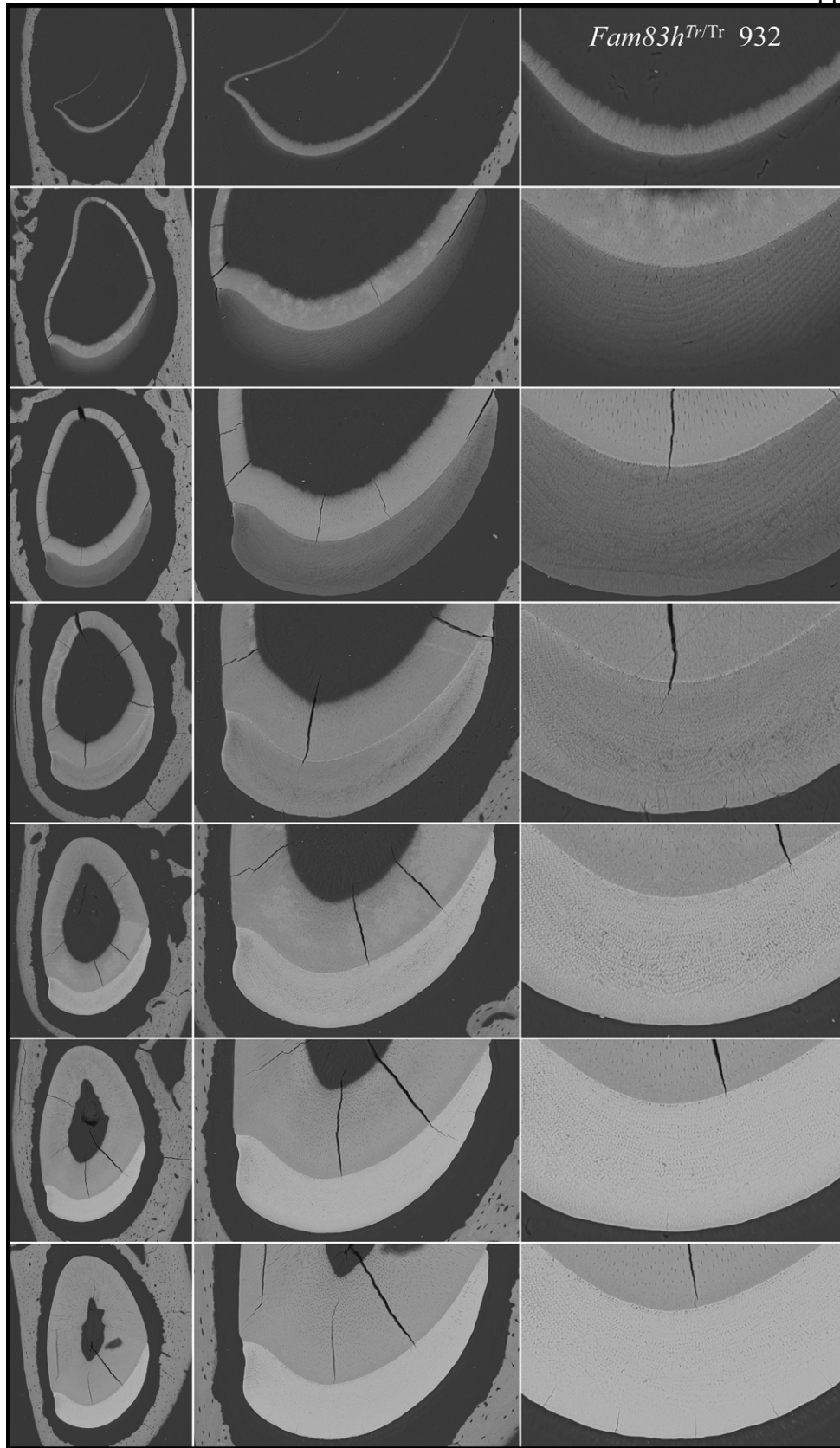


Fig. S17. Backscattered SEM images of mandibular incisor cross-sections of Null-932 taken at ~1 mm increments starting at the apical end of the incisor. The top row around the mid-secretory stage. The second row approximates the end of the secretory stage when the enamel layer reaches its final dimensions. Subsequent images show progressive mineralization of the enamel layer during the maturation stage.

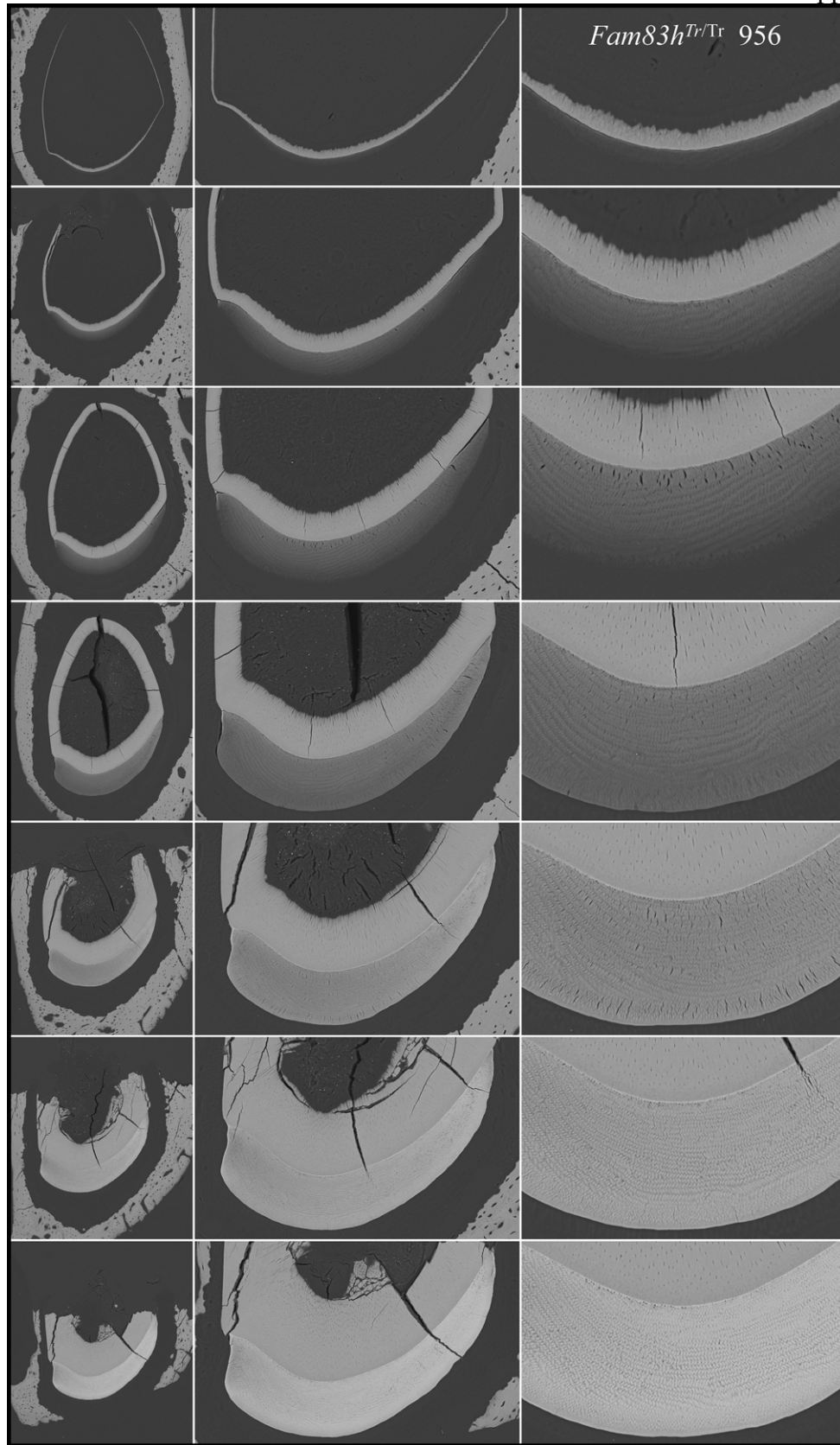


Fig. S18. Backscattered SEM images of mandibular incisor cross-sections of Null-956 taken at ~1 mm increments starting at the apical end of the incisor. The top row around the mid-secretory stage. The second row approximates the end of the secretory stage when the enamel layer reaches its final dimensions. Subsequent images show progressive mineralization of the enamel layer during the maturation stage.

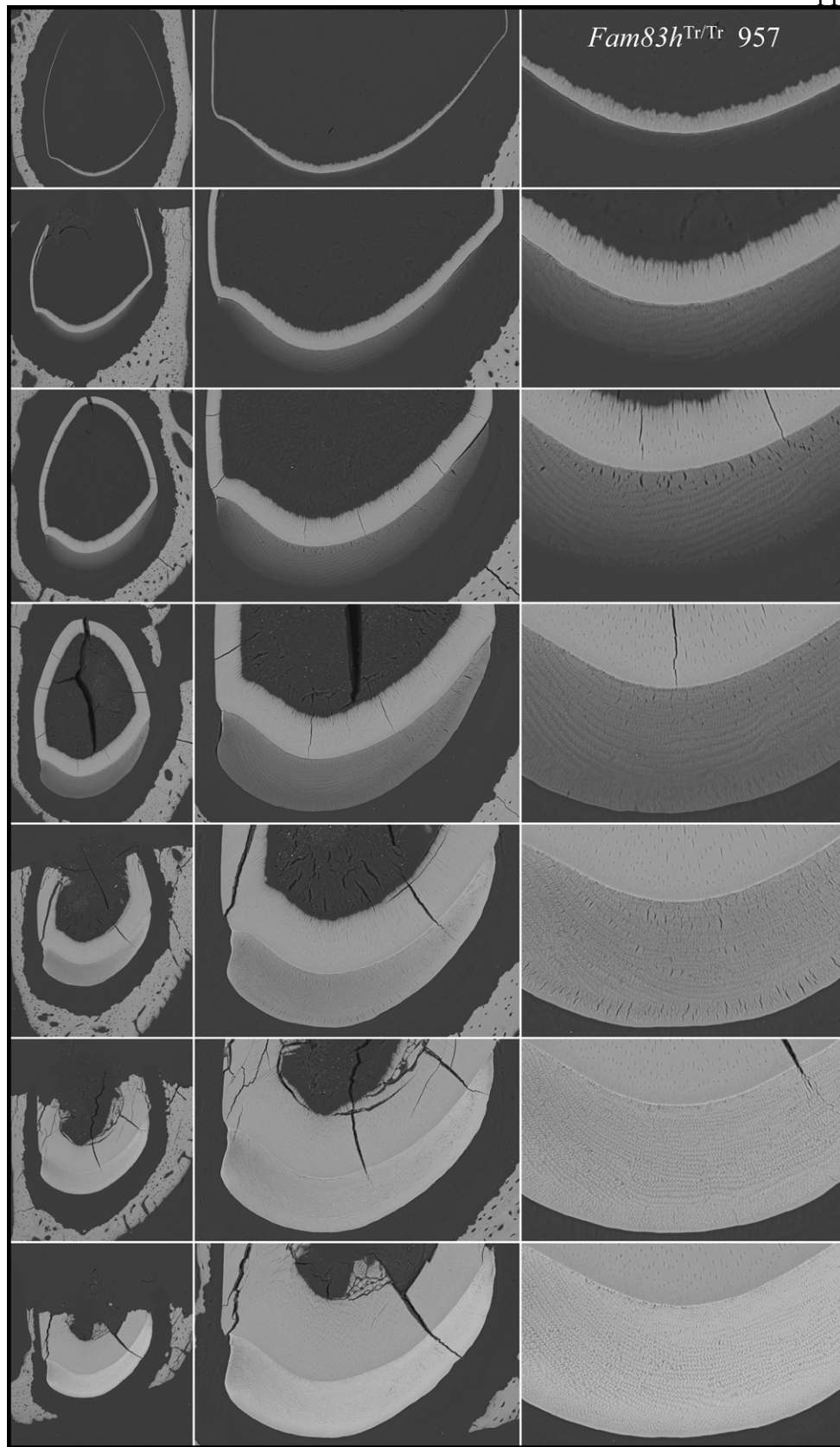


Fig. S19. Backscattered SEM images of mandibular incisor cross-sections of Null-957 taken at ~1 mm increments starting at the apical end of the incisor. The top row around the mid-secretory stage. The second row approximates the end of the secretory stage when the enamel layer reaches its final dimensions. Subsequent images show progressive mineralization of the enamel layer during the maturation stage.

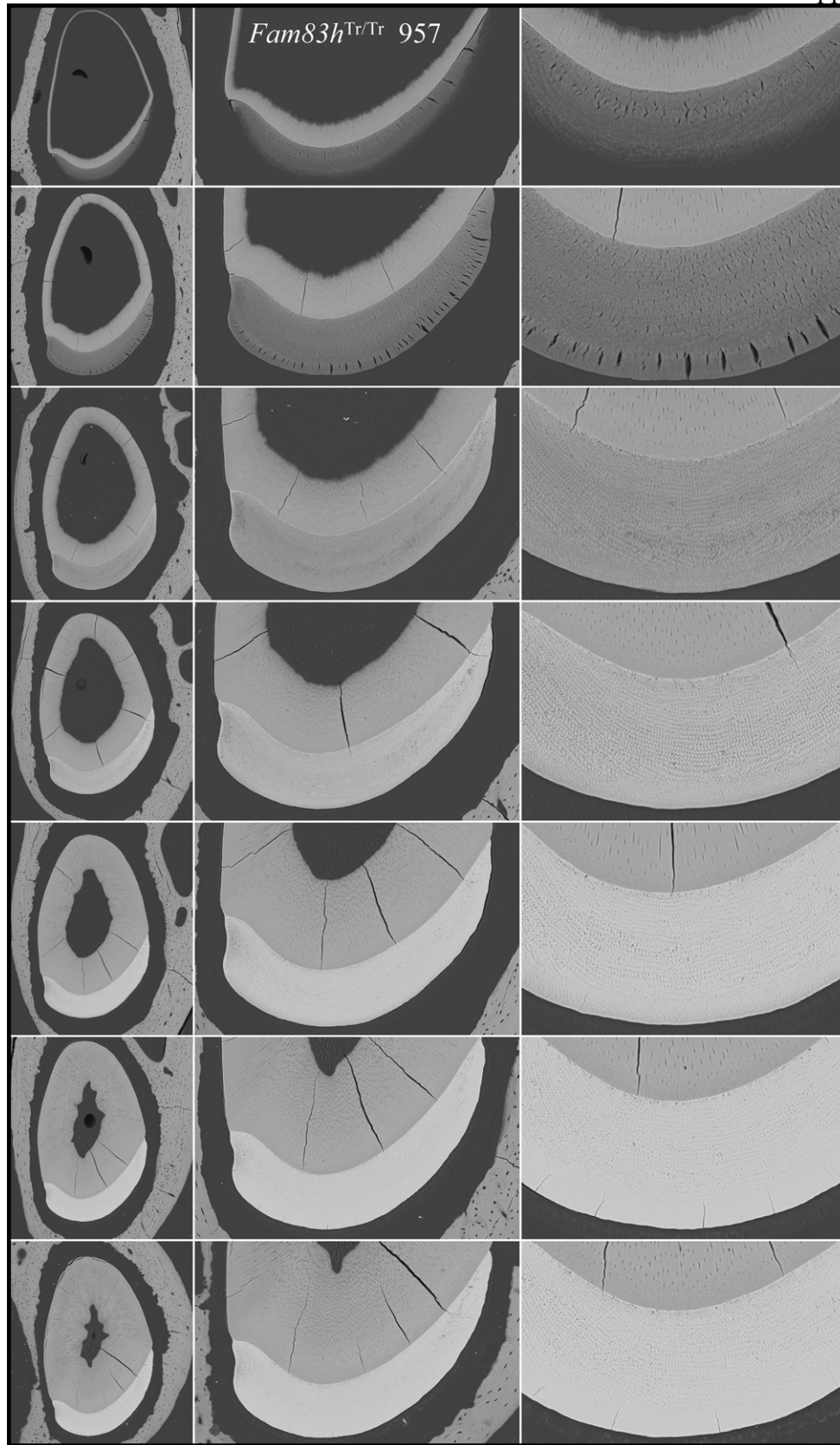


Fig. S20. Backscattered SEM images of mandibular incisor cross-sections of Null-974 taken at ~1 mm increments starting at the apical end of the incisor. The top row around the mid-secretory stage. The second row approximates the end of the secretory stage when the enamel layer reaches its final dimensions. Subsequent images show progressive mineralization of the enamel layer during the maturation stage.

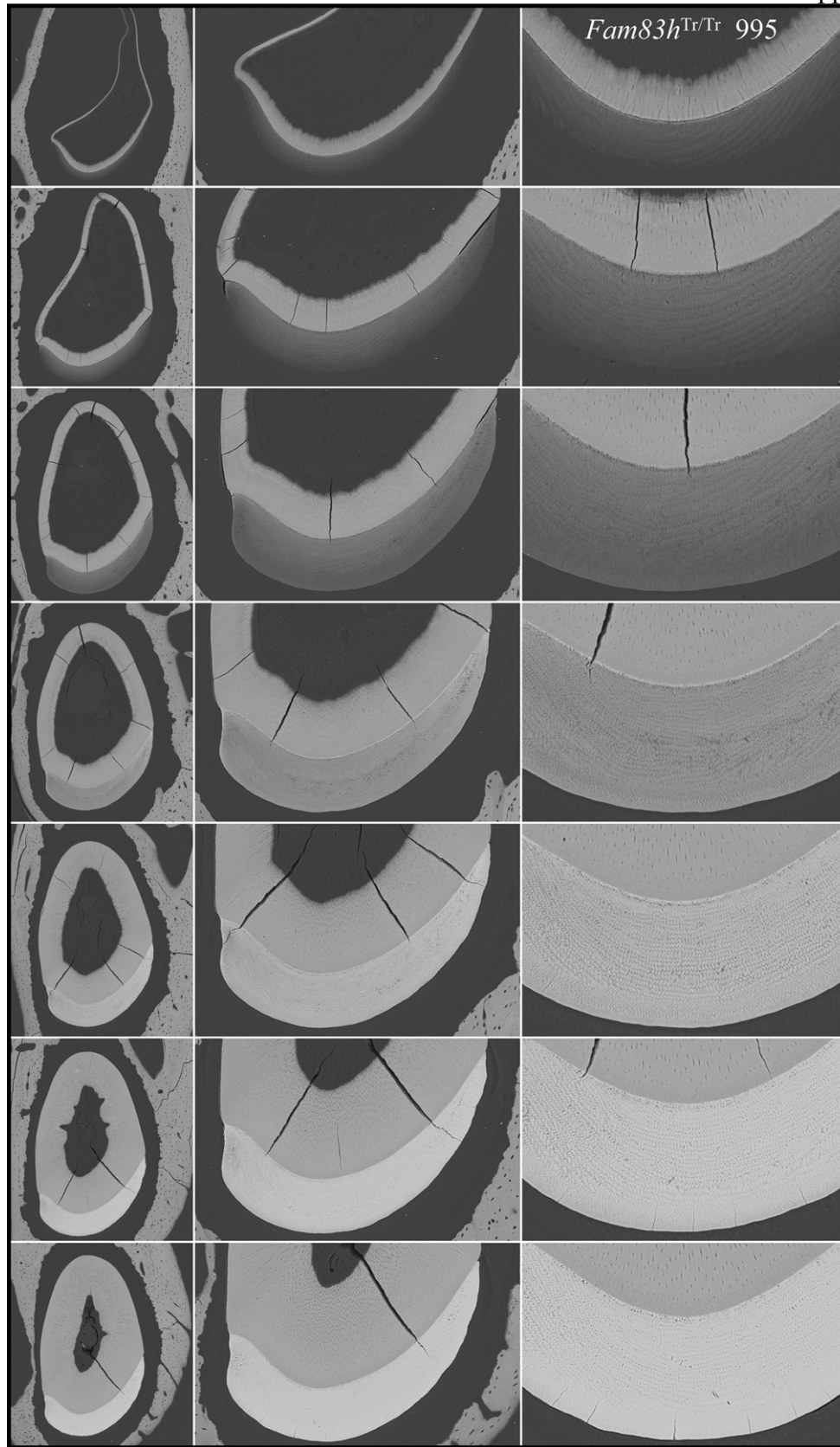


Fig. S21. Backscattered SEM images of mandibular incisor cross-sections of Null-995 taken at ~1 mm increments starting at the apical end of the incisor. The top row around the mid-secretory stage. The second row approximates the end of the secretory stage when the enamel layer reaches its final dimensions. Subsequent images show progressive mineralization of the enamel layer during the maturation stage.

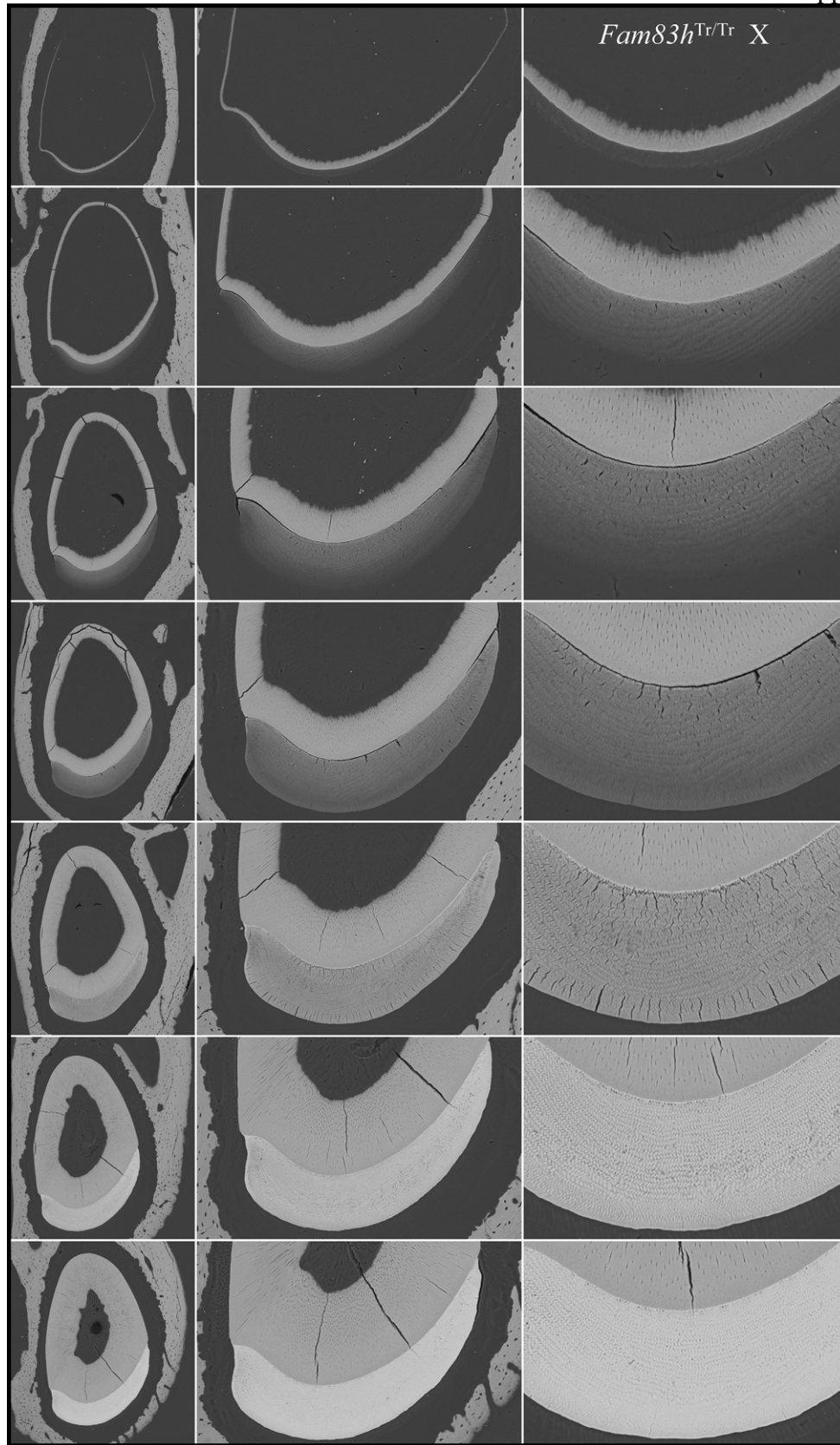


Fig. S22. Backscattered SEM images of mandibular incisor cross-sections of Null-X taken at ~1 mm increments starting at the apical end of the incisor. The top row around the mid-secretory stage. The second row approximates the end of the secretory stage when the enamel layer reaches its final dimensions. Subsequent images show progressive mineralization of the enamel layer during the maturation stage.

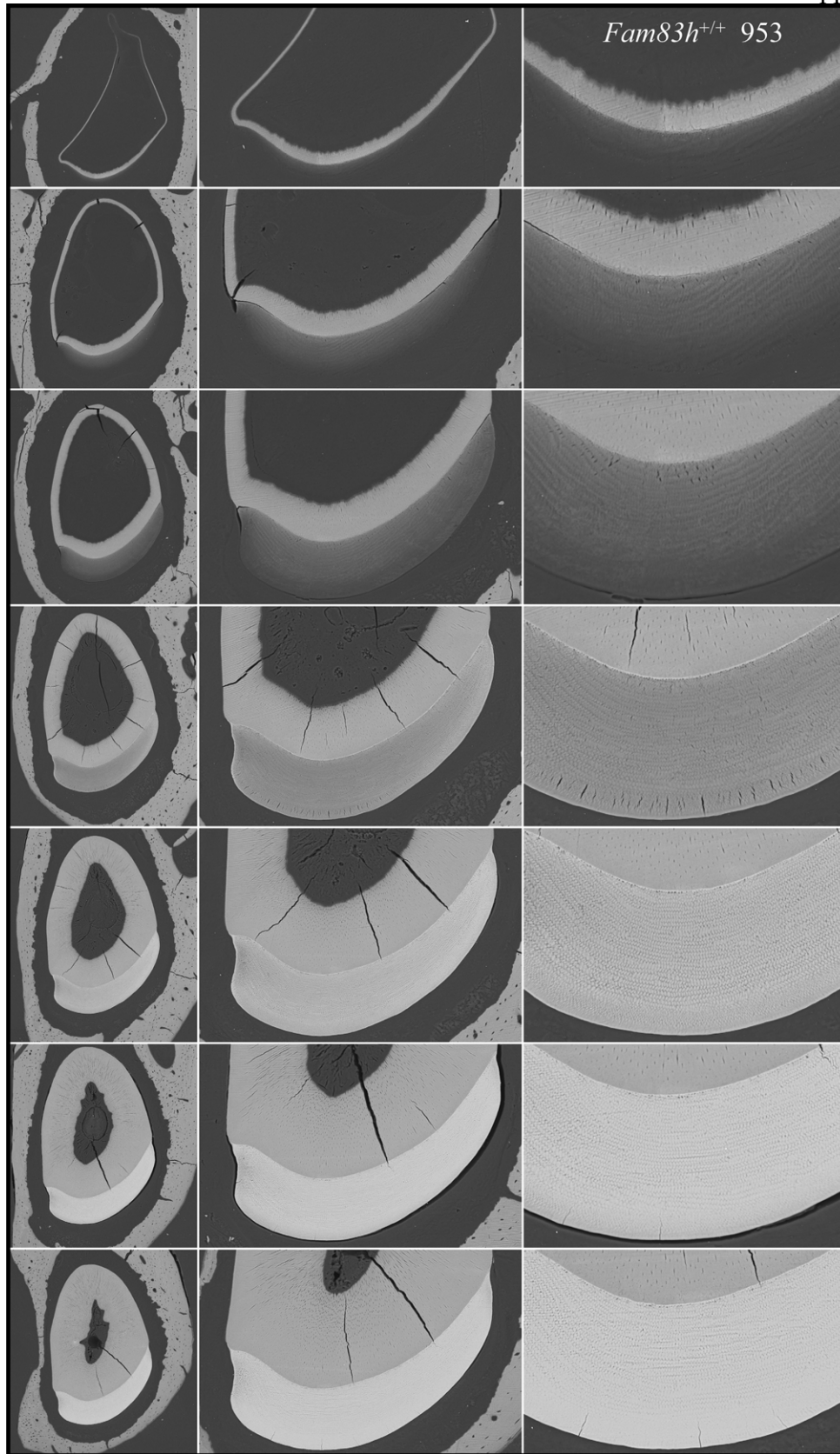
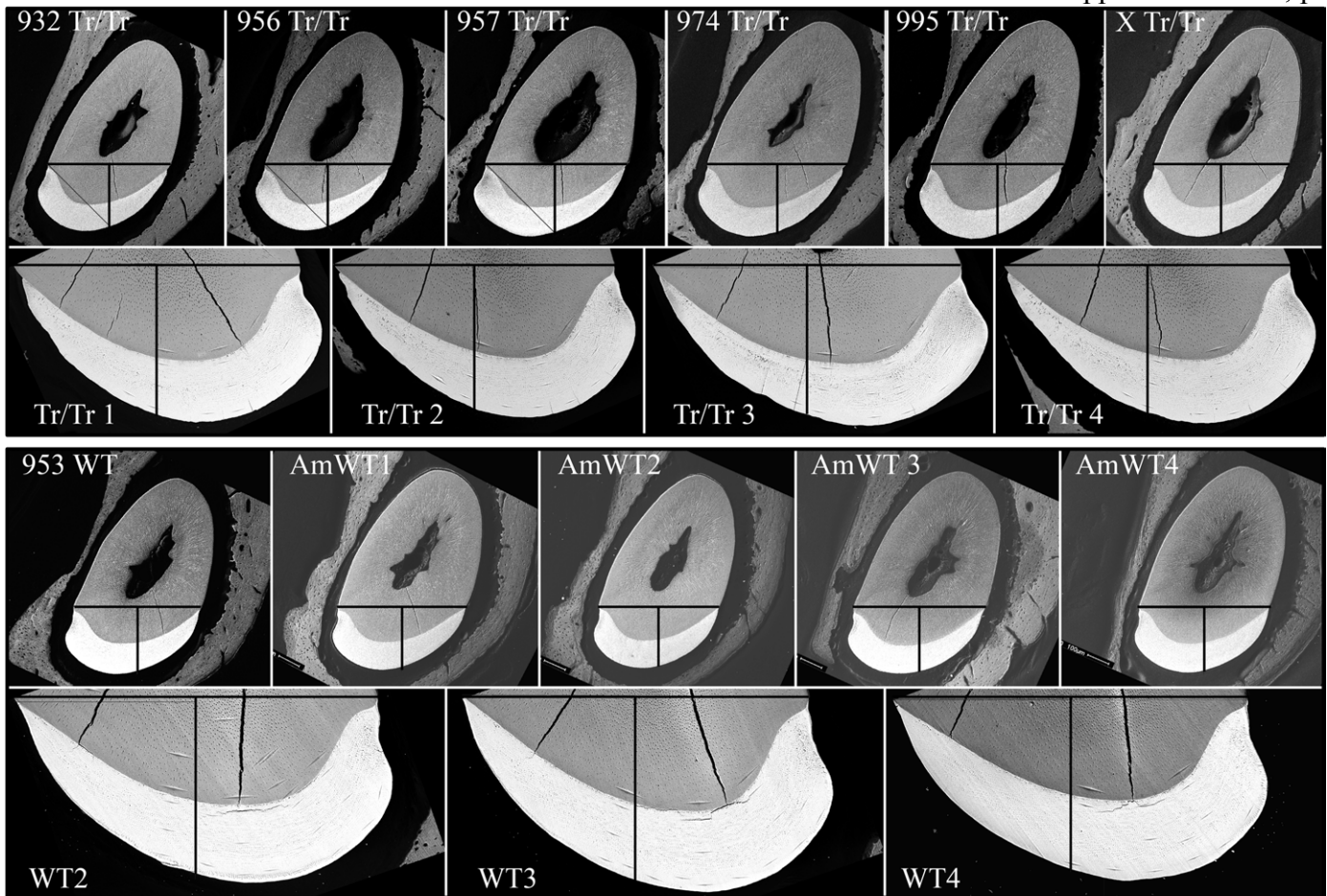
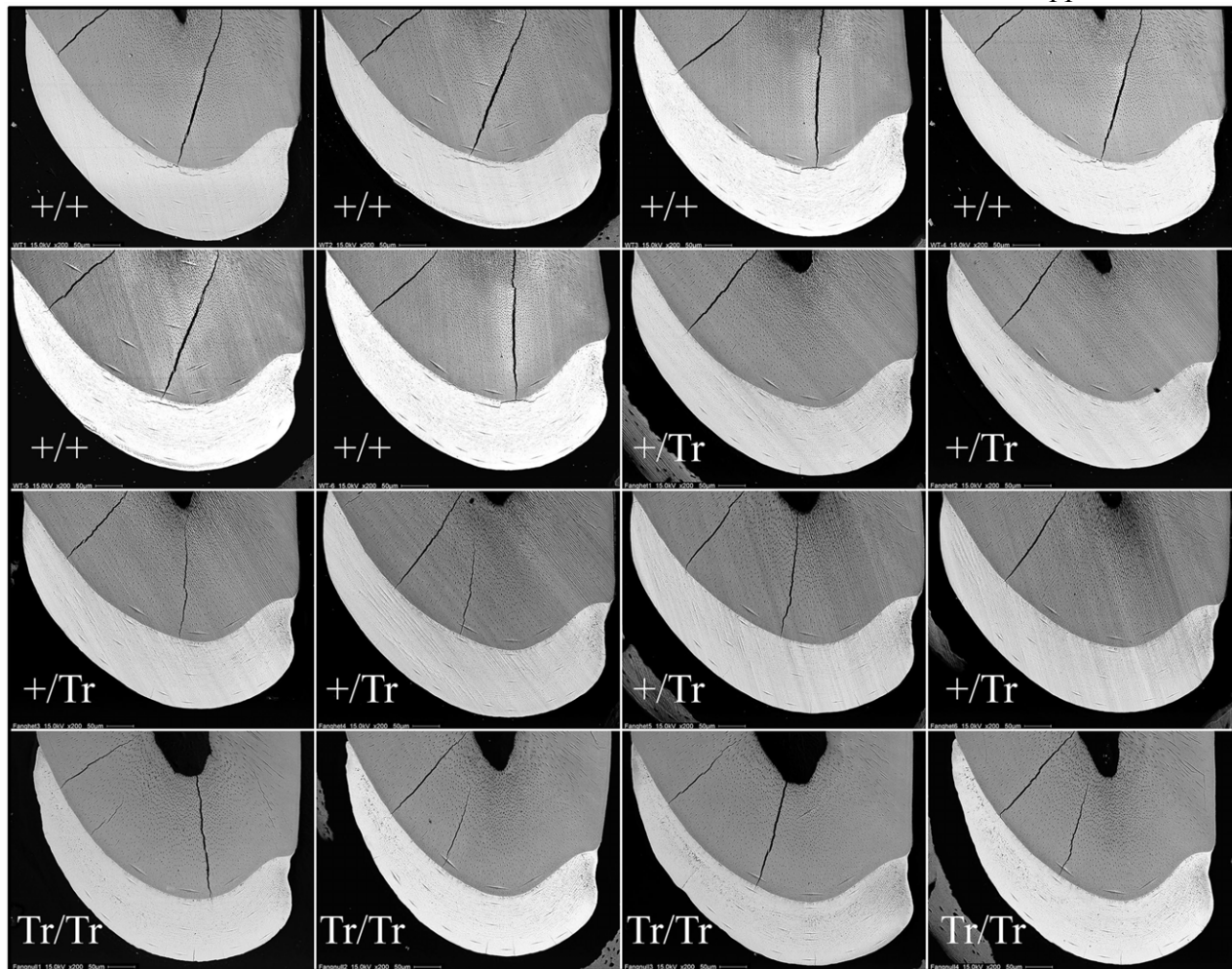


Fig. S23. Backscattered SEM images of mandibular incisor cross-sections of Wild-Type-953 taken at ~1 mm increments starting at the apical end of the incisor. The top row around the mid-secretory stage. The second row approximates the end of the secretory stage when the enamel layer reaches its final dimensions. Subsequent images show progressive mineralization of the enamel layer during the maturation stage.



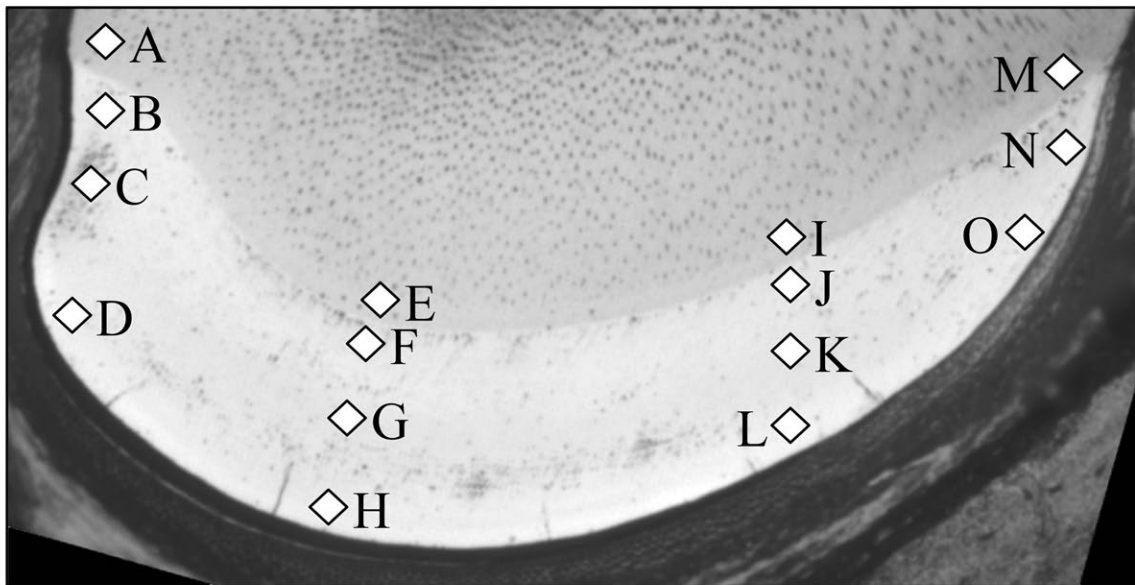
Null Enamel Area (μm^2)				WT Enamel Area (μm^2)			
Sample	Lateral	Medial	Whole	Sample	Lateral	Medial	Whole
932 Tr/Tr	24199.0	48075.8	72274.8	953 WT	28866.7	49745.9	78612.6
956 Tr/Tr	23267.1	45422.8	68689.9	AmWT1	28061.2	44297.2	72358.4
957 Tr/Tr	24462.1	45471.8	69933.8	AmWT2	27055.9	41046.7	68102.6
974 Tr/Tr	21119.8	44743.8	65863.6	AmWT3	29156.3	45730.7	74887.0
995 Tr/Tr	23628.0	45245.4	68873.4	AmWT4	31519.7	46173.2	77692.9
X Tr/Tr	21988.5	44717.3	66705.8	WT2	26009.9	44452.2	70462.1
Tr/Tr 1	21158.0	42020.5	63178.4	WT3	27673.6	46970.4	74644.0
Tr/Tr 2	20085.6	40199.4	60285.0	WT4	26654.9	46210.9	72865.9
Tr/Tr 3	21630.0	45227.8	66857.8				
Tr/Tr 4	21085.9	43971.5	65057.4				
Average	22262.4	44509.6	66772.0	Average	28124.8	45578.4	73703.2
STDEV	1512.4	2126.4	3450.3	STDEV	1737.1	2493.7	3519.1

Fig. S24. Enamel area on 7-week mandibular incisor level 8 (alveolar crest) cross sections. The enamel was divided into mesial and lateral regions by drawing a line from the mesial cervical margin to the lateral cervical margin and drawing a perpendicular from its midpoint. The mesial, lateral, and total cross-sectional areas (mm^2) were determined by outlining the enamel on Photoshop (*Fam83h*^{+/+} n=8; *Fam83h*^{Tr/Tr} n=10). All p values were below 0.01 were considered to be significant. Significant differences were observed between the wild-type and the *Fam83h* homozygous truncation (*Fam83h*^{Tr/Tr}) incisors in their lateral and total cross-sectional areas, but not in the mesial enamel.



	+/+	+/+	+/+	+/+	+/+	+/+	Ave
Dentin	142.6	142.8	123.9	133.4	139.1	124.4	134.4± 8.6
Inner	307.6	337.0	250.4	302.4	347.8	299.4	307.4± 34.2
Middle	369.3	358.6	342.8	366.1	355.0	335.6	354.6± 13.1
Outer	356.4	354.9	347.6	340.6	363.8	358.9	353.7± 8.3
	+/Tr	+/Tr	+/Tr	+/Tr	+/Tr	+/Tr	Ave
Dentin	124.0	122.6	120.2	143.5	128.8	133.2	128.7± 8.6
Inner	262.3	259.6	268.5	186.5	250.4	308.3	255.9± 39.5
Middle	321.8	349.2	331.9	373.7	330.0	338.1	340.8± 18.5
Outer	391.0	354.9	361.6	395.5	386.2	373.8	377.2± 16.5
	Tr/Tr	Tr/Tr	Tr/Tr	Tr/Tr			Ave
Dentin	141.0	131.2	133.0	136.8			135.5± 4.3
Inner	312.0	300.0	299.5	307.7			304.8± 6.2
Middle	351.2	345.6	336.1	354.1			346.7± 7.9
Outer	85.9	389.1	339.5	391.2			376.4± 24.7

Fig. S25. Microhardness Testing. **Top:** bSEM images of 7-week mandibular incisor cross sections from level 8 (where the incisor has erupted to the alveolar crest). This level is chosen because the tooth is in an advanced state of maturation but has not entered the oral cavity where it could be weakened by occlusal forces. *Fam83h*^{+/+} (n=6), *Fam83h*^{+/Tr} (n=6) and *Fam83h*^{Tr/Tr} (n=4) mice. **Bottom:** Table showing the average values with standard deviations for each sample.



	Dentin			Middle Enamel			
	WT	<i>Fam83h</i> ^{+Tr}	<i>Fam83h</i> ^{Tr/Tr}	WT	<i>Fam83h</i> ^{+Tr}	<i>Fam83h</i> ^{Tr/Tr}	
A	1.24±0.07	1.23±0.06	1.40±0.33	G	3.43±0.16	3.29±0.19	3.47±0.37
E	1.12±0.05	1.14±0.11	1.24±0.26	K	3.52±0.11	3.15±0.21	3.17±0.51
I	1.10±0.04	1.08±0.10	1.30±0.31		(excluded)		
M	1.32±0.08	1.26±0.13	1.34±0.26	C	1.44±0.45	1.35±0.60	1.40±0.26
	Inner Enamel			Outer Enamel			
	WT	<i>Fam83h</i> ^{+Tr}	<i>Fam83h</i> ^{Tr/Tr}	WT	<i>Fam83h</i> ^{+Tr}	<i>Fam83h</i> ^{Tr/Tr}	
B	2.59±0.70	2.58±0.72	2.31±0.60	D	3.53±0.15	3.12±0.19	3.12±0.65
F	3.05±0.38	2.65±0.20	3.06±0.66	H	4.18±0.19	4.07±0.20	3.92±0.57
J	3.20±0.20	3.02±0.47	3.42±0.16	L	3.79±0.12	3.76±0.21	3.96±0.51
N	3.48±0.07	2.78±0.71	3.06±0.72	O	3.61±0.19	3.58±0.17	3.76±0.16

Fig. S26. Nanohardness Testing. Top: Locations of 15 nano-indents labeled A through O made in level 8 cross-sections of 7-week mandibular incisors in *Fam83h*^{+/+} (n=6), *Fam83h*^{+Tr} (n=6) and *Fam83h*^{Tr/Tr} (n=5) mice. **Bottom:** Table showing the average values with standard deviations for each indent position. The values in Fig. 6 are averages of these values: dentin = averages of the hardness values from indents at locations A, E, I and M (24 indents each for *Fam83h*^{+/+} and *Fam83h*^{+Tr}, 20 indents for *Fam83h*^{Tr/Tr}); Inner Enamel = averages from locations B, F, J, and N (24 indents each for *Fam83h*^{+/+} and *Fam83h*^{+Tr}, 20 indents for *Fam83h*^{Tr/Tr}); Middle Enamel = averages from locations G and K (12 indents each for *Fam83h*^{+/+} and *Fam83h*^{+Tr}, 10 indents for *Fam83h*^{Tr/Tr}; note: indents from location C were not included because of high variations in enamel hardness at this location); Outer Enamel = averages from locations D, H, L, and O (24 indents each for *Fam83h*^{+/+} and *Fam83h*^{+Tr}, 20 indents for *Fam83h*^{Tr/Tr}).

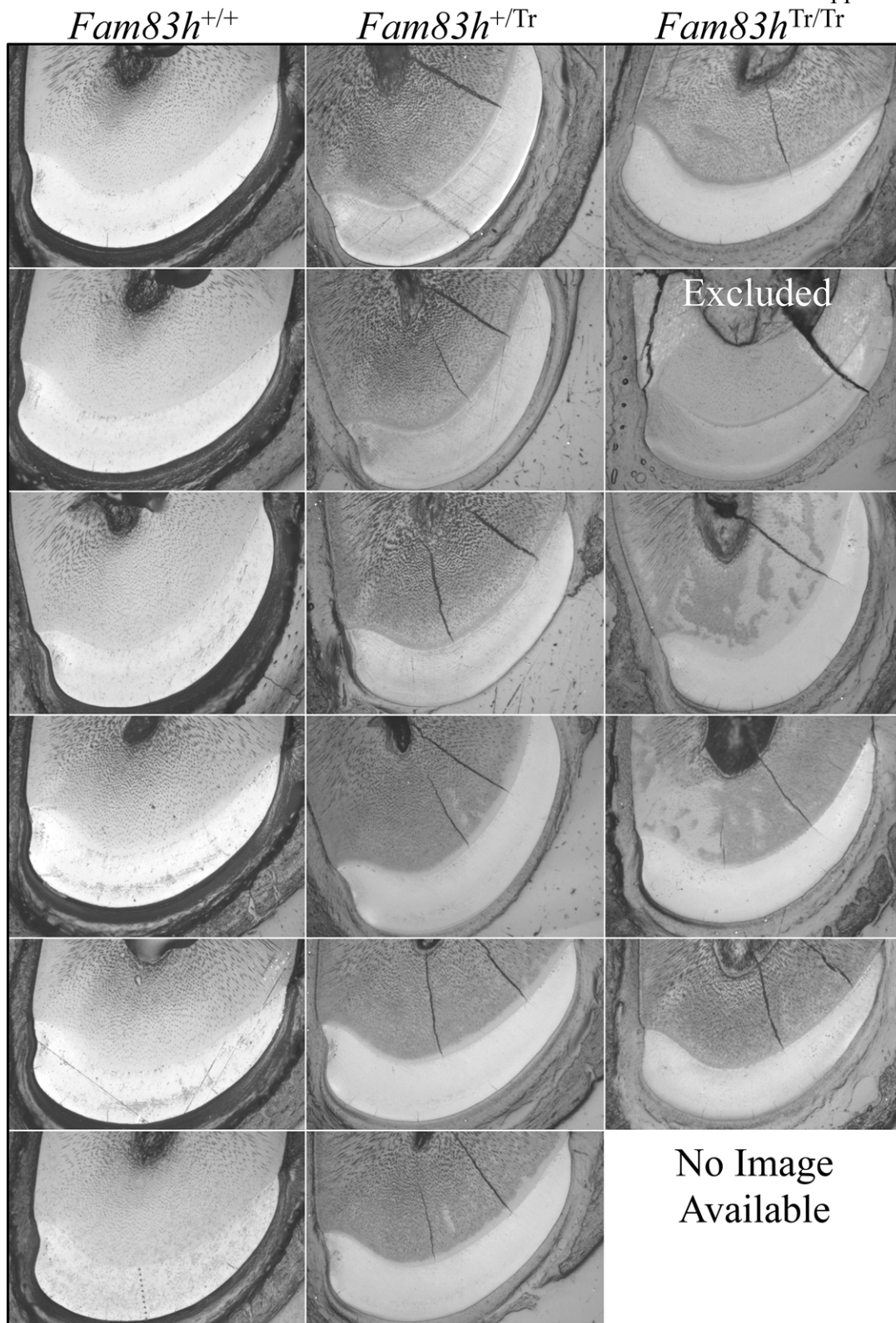


Fig S27. Nanohardness Testing. SEM images of level 8 cross-sections of 7-week mandibular incisors in *Fam83h*^{+/+} (n=6), *Fam83h*^{+/Tr} (n=6) and *Fam83h*^{Tr/Tr} (n=5) mouse samples used for nanohardness testing.